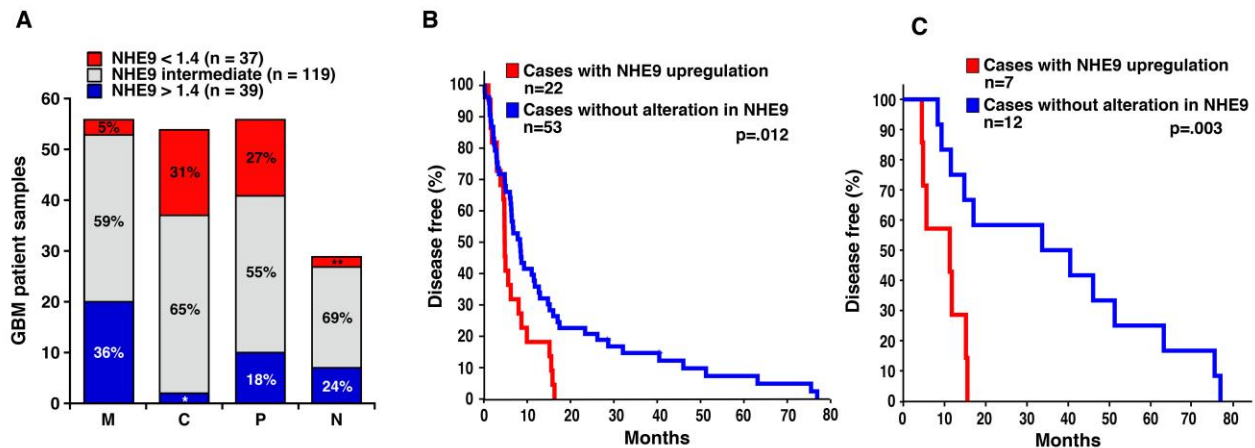


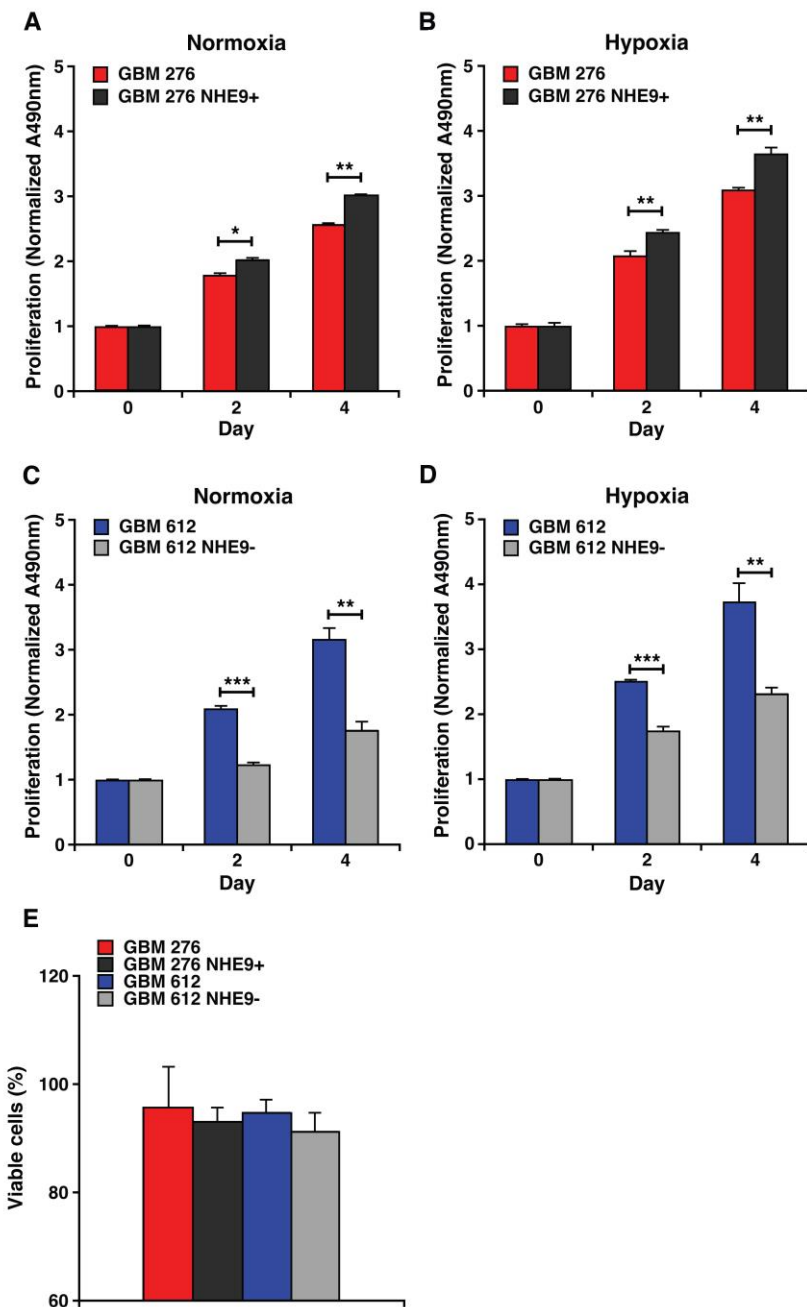
Supplementary Figure 1



Supplementary Figure 1. Correlation of NHE9 expression with GBM subtype and patient survival

(A) Microarray expression data of NHE9 were analyzed and sorted according to glioblastoma subtype classification (M, mesenchymal; C, classical; P, proneural; N, neural) taken from the Glioblastoma TCGA dataset (*, 4%; **, 7%; n = 185). Samples expressing NHE9 > 1.4 fold (n = 39) were overrepresented in the mesenchymal subgroup (36%). (B-C) NHE9 transcripts were up regulated in 28.6% of cases found in TCGA database using the cBio Cancer Genomics portal when a Z-score of 0.5 was selected. Patients with GBM up regulation of NHE9 had (B) shorter disease free periods after tumor resection ($p = 0.012$, Logrank test). A subset of patients with NHE9 upregulation who received neo-adjuvant chemotherapy showed drastically reduced disease free periods after resection when compared with patients expressing lower levels of NHE9 who received the same treatment (C) ($p = 0.003$; Logrank test).

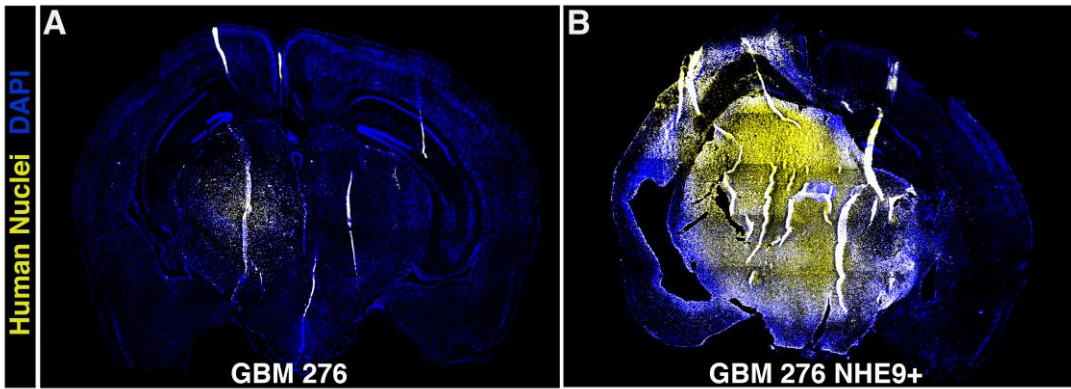
Supplementary Figure 2



Supplementary Figure 2. NHE9 expression correlates with BTIC proliferation under both normoxia and hypoxia but does not alter cell viability

Normalized proliferation of control GBM 276 and NHE9-overexpressing (276 NHE9+) under normoxia (A) or hypoxia (B) (** $p < 0.01$, * $p < 0.05$, two-tailed Welch's t-test, $n = 3$). Normalized proliferation of control GBM 612 and treated with NHE9 shRNA (612 NHE9-) under normoxia (C) or hypoxia (D) (** $p < 0.0001$, ** $p = 0.001$, two-tailed Welch's t-test, $n = 3$). MTS assay absorbance values were determined at 490 nm (A490nm). Bars represent mean \pm S.D. (E) Percentage of viable cells was measured by Trypan blue exclusion test after overexpression or knockdown of NHE9 in GBM 276 or 612, respectively. Bars represent mean \pm S.D.

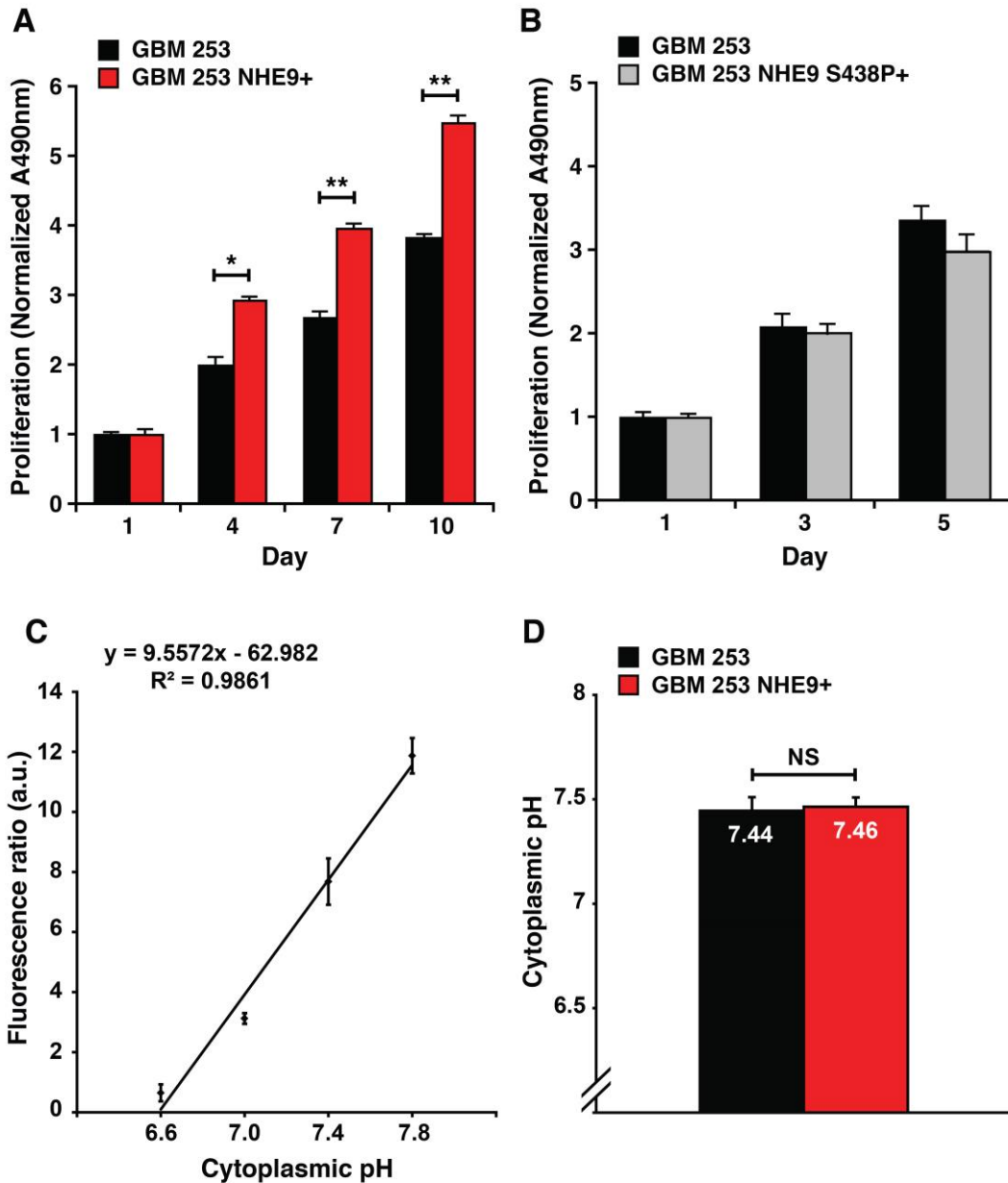
Supplementary Figure 3



Supplementary Figure 3: NHE9 expression increases in tumor growth and migration in vivo.

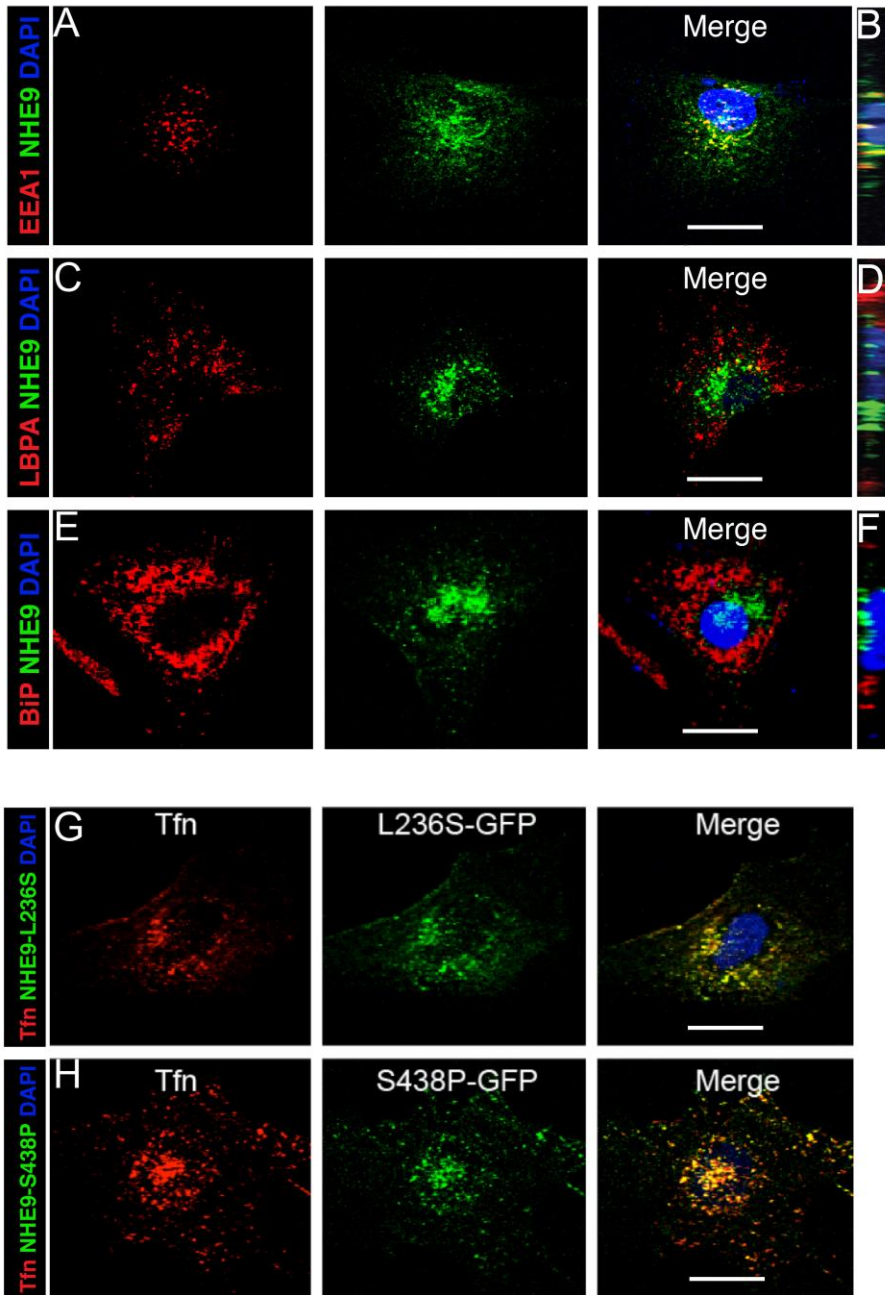
DAPI-stained coronal sections of mouse brains after injection of GBM 276 BTIC transfected with control shRNA (**A**) or NHE9 overexpression construct (**B**). Yellow staining represents human GBM cells identified by monoclonal IgG1 antibody against human nuclei.

Supplementary Figure 4



Supplementary Figure 4: Effect of NHE9 on proliferation and cytoplasmic pH of GBM 253(A) Normalized proliferation of control GBM 253 and NHE9-overexpressing (253 NHE9+) cells (** $p < 0.01$, * $p < 0.05$, two-tailed Welch's t-test, $n = 3$) as determined by MTS assay with absorbance values determined at 490 nm (A490nm). (B) NHE9 carrying the loss of function mutation S438P does not confer increase in cell proliferation in GBM 253. (C) Cytoplasmic pH was determined by measuring the fluorescence emission of BCECF at pH-sensitive and pH-insensitive wavelengths, and calibrated in buffers of known pH as described in Methods. (D) NHE9 overexpression does not alter cytoplasmic pH in GBM 253. Cytoplasmic pH was determined to be 7.44 in vector-transformed control cells and 7.46 in cells transfected with NHE9.

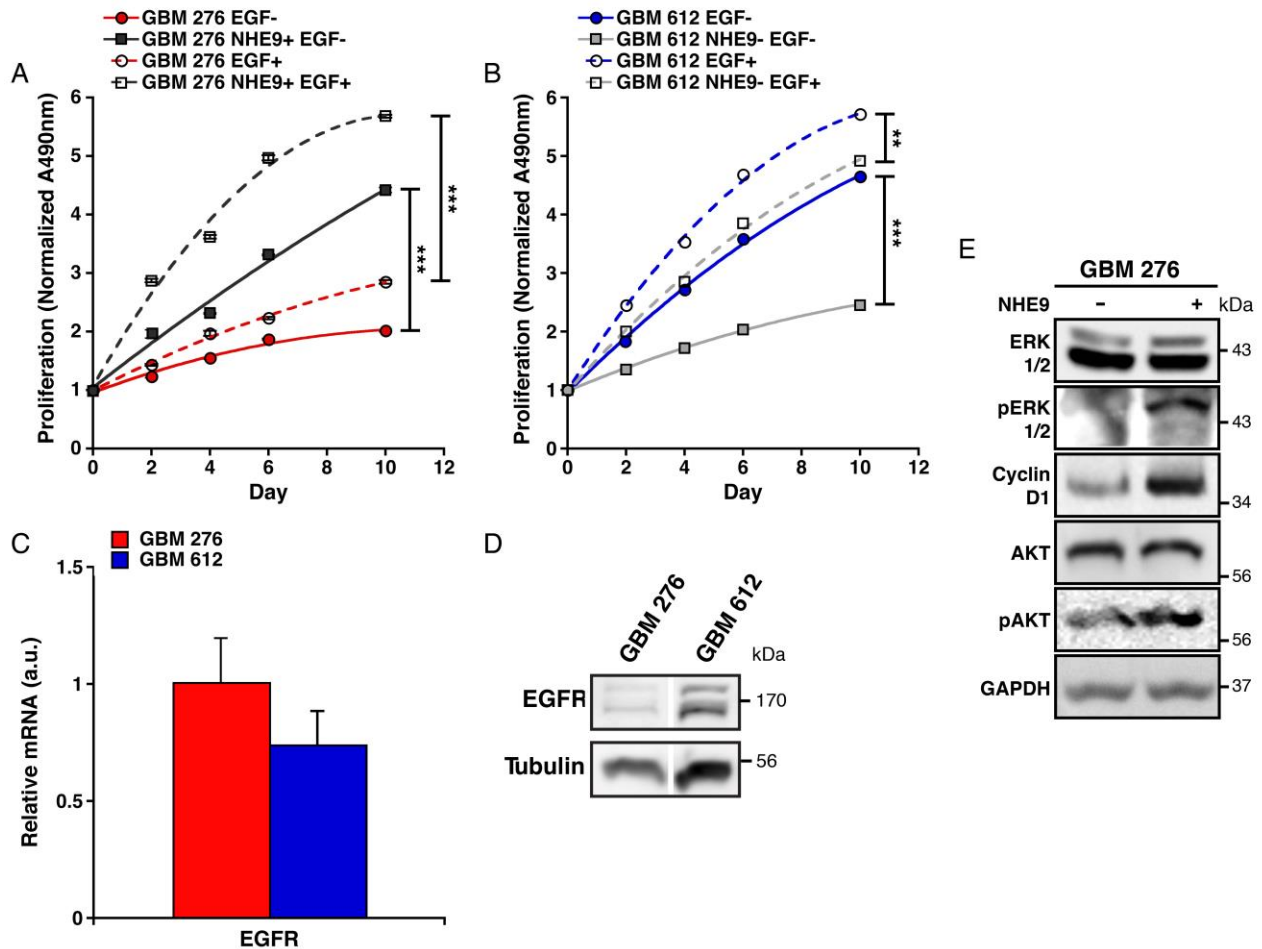
Supplementary Figure 5



Supplementary Figure 5. Subcellular localization of NHE9 in GBM 253 cells

Subcellular localization of NHE9 in GBM 253 cells determined by immunofluorescence confocal microscopy (63x objective) after fixation with 4% PFA. **(A)**, NHE9-GFP (*green*) partly localizes with early endosome marker, EEA1 (*red*) as seen in the Merge. NHE9-GFP (*green*) does not localize with late endosome marker, LBPA (*red*; **C**) or with the endoplasmic reticulum marker, BiP (*red*; **E**) as seen in the Merge. **(B, D, F)** Orthogonal views of subcellular localization of NHE9 from merged images in **A, C** and **E** respectively. NHE9 mutants (*green*) L236S (**G**) and S438P (**H**) colocalize with Tfn-633 (*red*). Scale bars: 20 μ m.

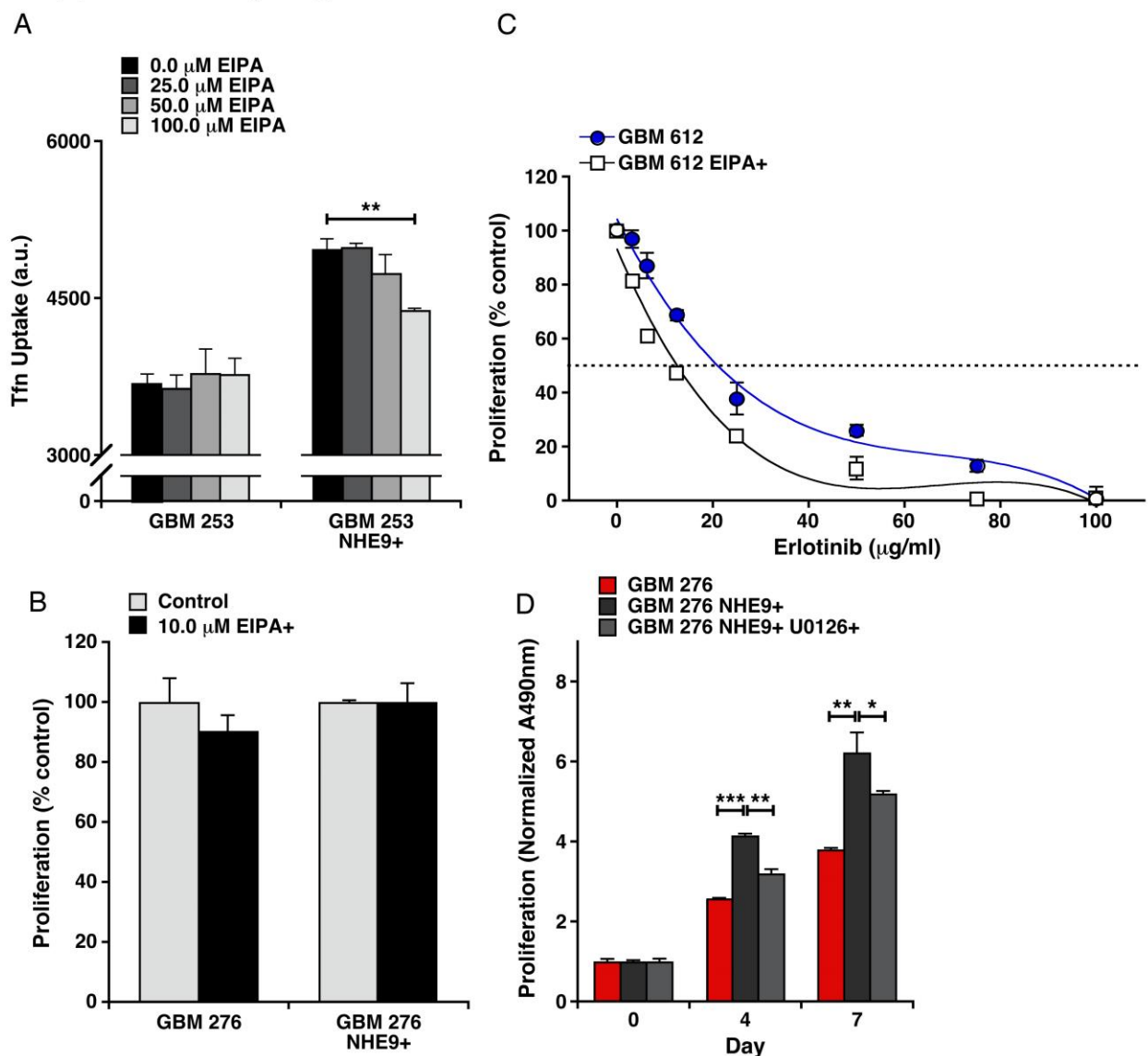
Supplementary Figure 6



Supplementary Figure 6. NHE9 drives EGFR membrane persistence and downstream oncogenic signaling in GBM BTIC

(A) GBM 276 control cells, NHE9 overexpressing cells were either cultured with or without EGF (20ng/ml) and cell proliferation was monitored for 10 days using MTS assay ($***p < 0.0001$, two-tailed Welch's t-test, $n = 3$). Absorbance values were determined at 490 nm (A490nm). (B) Same as in (A) GBM 612 control cells and 612 cells with shRNA knockdown of NHE9 ($***p < 0.0001$, $**p = 0.001$, two-tailed Welch's t-test, $n = 3$). (C) qPCR analysis of EGFR mRNA in cells from two primary GBM tumors 276, and 612 ($n = 3$). (D) Western blot of a surface biotinylation assay showing 2.92 fold higher plasma membrane level of EGFR (normalized to the loading control) in GBM 612 cells relative to GBM 276 cells run on the same Western blot. (E) Downstream signaling pathways of GBM 276 cells treated with EGF (30 min) were altered in cells overexpressing NHE9. Cell lysates were immunoblotted with the indicated antibodies.

Supplementary Figure 7



Supplementary Figure 7. Effects of pharmacological inhibition of NHE9 and MAP kinase on transferrin uptake and cell proliferation respectively

(A) Dose dependent reversal of the NHE9-mediated increase in transferrin uptake in GBM 253 cells by EIPA as determined by flow cytometry (** $p = 0.001$, two-tailed Welch's t-test, $n = 3$). (B) Low dose EIPA does not inhibit the growth of GBM cells. GBM 276 cells and GBM 276 overexpressing NHE9 were treated with vehicle or 10.0 μM EIPA for 24 hrs and cell viability was measured with a colorimetric MTS assay with absorbance values determined at 490 nm (A490nm). The graph shows proliferation of EIPA treated cells normalized to their respective nontreated control ($n = 3$). (C) EIPA enhances Erlotinib sensitivity of GBM 612 cells. GBM 612 cells were pretreated for 24 hrs with 85.83 $\mu\text{g/ml}$ (EIPA IC_{50} of 276 NHE9+ cells) or vehicle, followed by addition of EGFR inhibitor Erlotinib as indicated. Cell viability was measured by MTS assay ($n = 3$) after 24 hours. (D) MAP kinase functions downstream of NHE9 in GBM cell proliferation. Normalized proliferation of GBM 276 control cells and 276 cells overexpressing NHE9 and control cells treated with U0126, a known MAP kinase (ERK1/2) inhibitor (** $p < 0.0001$, ** $p = 0.001$, * $p < 0.05$, two-tailed Welch's t-test, $n = 3$) Bars represent mean \pm S.D.

Supplementary Table 1. Patient information corresponding to Glioblastoma BTIC.

Cell line	Diagnosis	Subtype	Age at resection	Gender	NHE9
GBM 276	Glioblastoma	Proneural	53	Female	+
GBM 253	Glioblastoma	Mesenchymal	53	Female	++
GBM 612	Glioblastoma	Mesenchymal	56	Female	++++